

University of Warwick institutional repository: <http://go.warwick.ac.uk/wrap>

This paper is made available online in accordance with publisher policies. Please scroll down to view the document itself. Please refer to the repository record for this item and our policy information available from the repository home page for further information.

To see the final version of this paper please visit the publisher's website. Access to the published version may require a subscription.

Author(s): Mudassar Iqbal, Yvonne Mast, Rafat Amin, David A. Hodgson, The STREAM Consortium, Wolfgang Wohlleben and Nigel J. Burroughs

Article Title: Extracting regulator activity profiles by integration of de novo motifs and expression data: characterizing key regulators of nutrient depletion responses in *Streptomyces coelicolor*

Year of publication: 2012

Link to published article:

<http://dx.doi.org/10.1093/nar/gks205>

Publisher statement: This is an Open Access article distributed under the terms of the Creative Commons Attribution Non-Commercial License (<http://creativecommons.org/licenses/by-nc/3.0>), which permits unrestricted non-commercial use, distribution, and reproduction in any medium, provided the original work is properly cited.

# Extracting regulator activity profiles by integration of *de novo* motifs and expression data: characterizing key regulators of nutrient depletion responses in *Streptomyces coelicolor*

Mudassar Iqbal<sup>1,\*</sup>, Yvonne Mast<sup>2</sup>, Rafat Amin<sup>2</sup>, David A. Hodgson<sup>3</sup>, The STREAM Consortium, Wolfgang Wohlleben<sup>2</sup> and Nigel J. Burroughs<sup>4,\*</sup>

<sup>1</sup>Multidisciplinary Centre for Integrative Biology (MyCIB), School of Biosciences, University of Nottingham, Nottingham, UK, <sup>2</sup>Department of Microbiology/Biotechnology, University of Tübingen, Germany, <sup>3</sup>School of Life Sciences and <sup>4</sup>Warwick Systems Biology Centre, University of Warwick, Coventry, CV4 7AL, UK

Received November 24, 2011; Revised February 14, 2012; Accepted February 15, 2012

## ABSTRACT

Determining transcriptional regulator activities is a major focus of systems biology, providing key insight into regulatory mechanisms and co-regulators. For organisms such as *Escherichia coli*, transcriptional regulator binding site data can be integrated with expression data to infer transcriptional regulator activities. However, for most organisms there is only sparse data on their transcriptional regulators, while their associated binding motifs are largely unknown. Here, we address the challenge of inferring activities of unknown regulators by generating *de novo* (binding) motifs and integrating with expression data. We identify a number of key regulators active in the metabolic switch, including PhoP with its associated directed repeat PHO box, candidate motifs for two SARPs, a CRP family regulator, an iron response regulator and that for LexA. Experimental validation for some of our predictions was obtained using gel-shift assays. Our analysis is applicable to any organism for which there is a reasonable amount of complementary expression data and for which motifs (either over represented or evolutionary conserved) can be identified in the genome.

## INTRODUCTION

A common theme of systems biology is to understand transcriptional regulation, i.e., to identify regulators

driving a particular function and to determine the activities of those transcription factors (TFs). A key problem, however, is that TFs are typically regulated (activated) at the protein level; thus their expression (mRNA) is not a reliable surrogate for their activity. Although there are methods to directly ascertain protein modifications, e.g., iTRAQ (1,2), these methods are unable to give a global coverage and typically only a few samples are available. Further, the targets of these TFs are often unknown; TF binding sites can be ascertained directly by ChIP-Seq/chip, but the proportion of functional binding sites is low at 50–58% (3,4), most likely due to the absence of (unexpressed) codependents under the experimental conditions. Because of these problems, computational techniques have emerged to infer both the regulatory network and the associated activity of the specified regulators/TFs (3–9). A comparison of some of these methods were performed in (10). These methods combine gene expression data with TF binding site information, either predicted from a known motif or using ChIP-Seq/chip data. Essentially by restricting the network to the implied binding targets, expression data can be used to infer the activity of the associated TF. These methods perform best with high volumes of expression data, being able to utilize both steady state and time-series data. As such they are ideal methods for integration of data sets. However, all these methods are restricted to highly studied organisms such as *Escherichia coli*, *Schizosaccharomyces pombe* and *Drosophila*. To address TF/regulator activity in poorly studied organisms we present a generic method to infer regulator activities designed for when neither the regulators nor their binding motifs are known. The method integrates expression data

\*To whom correspondence should be addressed. Tel: +44 (0)115 951 6549; Fax: +44 (0)115 9516 261; Email: mudassar.iqbal@nottingham.ac.uk  
Correspondence may also be addressed to Nigel Burroughs. Tel: +44 (0)24 76524682; Fax: +44 (0)24 76575795; Email: n.j.burroughs@warwick.ac.uk

with the genome sequence. It generalizes the above methods, inferring activities of *de novo* identified motifs from their target gene expression profiles. The requirements are a sequenced genome for which a *de novo* search of motifs is successful and a reasonable quantity of gene expression data (e.g. >50 arrays). Motifs can be detected either because of their over representation in the genome or because they are evolutionarily conserved. These motifs are used to define potential regulatory connections between the (unknown) TFs/regulators and their targets; the expression data is then used to trim the network into active and inactive (or false) binding sites with a concurrent inference of the activity of the associated regulators.

Our analysis is based on a modification of the model of Sabatti and James (6); itself based on a commonly used statistical model for determining explanatory variables through pattern identification, specifically a factor model. Gene expression is modelled as a linear regression on the activity of a small number of unknown factors—in our case the motif activities—

$$e_{it} = \sum_j a_{ij} p_{jt} + \gamma_{it} \quad (1)$$

where  $e_{it}$  is the expression of gene  $i$ ,  $p_{jt}$  the (unknown) activity of TF  $j$ , both at time  $t$ ,  $a_{ij}$  the control strength of the transcriptional regulator through motif  $j$  on gene  $i$ , and  $\gamma_{it}$  Gaussian noise, assumed homogeneous in time but possibly gene specific. Connectivity is given by the connectivity matrix  $z_{ij}$  with  $z_{ij} = 1$  implying that the TF associated with motif  $j$  regulates gene  $i$ ; this is only possible if motif  $j$  lies in the upstream region of gene  $i$ . Then  $a_{ij}$  is zero if  $z_{ij} = 0$ . We implemented our model using a Markov chain Monte Carlo (MCMC) methodology, see [Supplementary Data](#).

We applied our method to an important soil bacterium *Streptomyces coelicolor*, a model organism in the actinomycetes, a phylum that is responsible for the production of most of the antibiotics currently in use. *Streptomyces coelicolor* initiates production of antibiotics under nutrient depletion (11,12), undergoing a so-called metabolic switch (13) from primary metabolism (and growth), to secondary metabolism, producing a rich array of metabolites including up to four antibiotics. Despite decades of research the complex regulatory mechanisms responsible for the metabolic switch are largely unknown. This organism has 66 sigma factors and over 700 potential DNA binding regulators ([Supplementary Table 8](#)), while very few binding motifs are known. The list of known binding motifs includes a PHO box of the phosphate response regulator PhoP (SCO4230) (14–16), a key regulator in the response to limited phosphate; the DasR binding motif, a global regulator of carbon utilization (17); ARE-sequence binding sites of key regulators such as ScbR (18) that regulate secondary metabolism pathways; binding sites for pathway-specific regulators of the SARP family (19,20); an inferred binding motif for the sigma factor  $\sigma^R$  (SCO5216) (21), a key regulator in sensing oxidative stress; and binding sites for GlnR (SCO4159) (22). In our study we examined computational

predictions for both evolutionary conserved motifs within the actinomycetes and over represented sequences in the genome. We found that over represented binding sites of the dyad type, i.e., two conserved sequences with a variable spacer between them, [a common pattern in bacterial genomes (23–26)], to be the most informative and only report on these in the following.

This article is organized as follows. In ‘Materials and Methods’ section, we describe the data sets, motif prediction, enrichment methodology, and factor model for integration of sequence and expression datasets. Also the experimental verification method is outlined. In ‘Results’ section, we enumerate the number of motif hits and implement a filtering/enrichment process to determine the informative motifs. On applying the factor model we find 10 distinct motif activity profiles/clusters supporting 61% of the target binding sites. We examine the overlap between target sets among motifs with similar activity profiles, detecting cases at both extremes—specifically, cases where the motifs model the same binding site, and where there is no target or motif correlation. In ‘Discussion’ section, we discuss the key motifs and their profiles. To determine the identity of the regulator we examine if there is any obvious homology of the motif to known bacterial motifs or if there are any regulators with expression profiles similar to the inferred activity profile.

## MATERIALS AND METHODS

### Gene expression data, differentially expressed genes

Gene expression data from three time series were used, **TS1**: wild-type under phosphate depletion (27), **TS3**: a *phoP* knock-out under phosphate depletion (M. Juarez *et al.*, submitted for publication), and **TS5**: the wild-type under glutamate depletion (28). There were 94 times points in total. Normalization was performed using RMA. For each of the time series we determined the differentially expressed (DE) genes using BATS software (29) and clustered the DE genes in each TS using splinecluster (30).

### Motif prediction and enrichment analysis

Upstream regions of genes (up to 300 bp) in the *S. coelicolor* genome (NCBI, <http://www.ncbi.nlm.nih.gov/>) (31) were used to search for over represented dyads using the software pipeline of (24). Using the operon definitions of ref. (32), we associate a motif located in the upstream regions of any of the genes within an operon with all genes in the operon. We used a hyper-geometric test to determine significant enrichment of dyad motifs in the DE genes and the expression profile clusters. To correct for multiple testing we used a Benjamini and Hochberg correction. Further details are given in [Supplementary Data](#).

### Factor model: integrating motif and expression data

We modified the hierarchical factor model of (6) and the associated MCMC algorithm for use on *S. coelicolor*. The underlying network model is a two-layered bipartite

network where edges are between regulators and their target genes as shown in [Supplementary Figure S2](#). We use a Bayesian methodology for the inference of the model parameters, i.e., matrices  $A$ ,  $P$ , noise variance  $\sigma_i^2$  as well as network structure (connectivity matrix  $Z$ ), Equation 1 (we use lowercase to denote elements of a matrix). Gibbs variable selection is used to infer the significant links (those with  $z_{ij} = 1$ ) in the network topology. The motif predictions are used as prior information restricting the possible regulatory links as (6), i.e.,  $z_{ij}$  is a random variable with  $z_{ij} \in \{0, 1\}$  iff motif  $j$  lies upstream of gene  $i$  (or is in the operon of  $i$ ), otherwise  $z_{ij} = 0$ . We implemented both an MCMC and Metropolis Coupled MCMC algorithm to sample the posterior distribution of the model parameters. The latter overcame the slow mixing of the network topology variables  $Z$  which was a particular issue in this high GC organism. Convergence was assessed using multiple chains. Matlab code for the factor model is available from MI on request.

### Electromobility shift assays

DNA fragments of genes of 100–250 bp upstream were amplified by PCR using genomic DNA of *S. coelicolor* M145 (genes and primers listed in [Supplementary Table 7](#)) and used for electromobility shift assay (EMSA) with *S. coelicolor* cell lysate under various culture conditions, see [Supplementary Data](#).

## RESULTS

We used the factor model, Equation 1 on data for the bacterium *S. coelicolor*, strain M145 (33), to determine the key regulator activity profiles and their associated regulatory motifs during the metabolic switch (13). Our expression data comprises three extended high-resolution longitudinal time series, TS1, TS3, TS5 that map the transcriptome over the switch from primary to secondary metabolism under nutrient depletion (phosphate or glutamate, see ‘Materials and Methods’ section). Between the three time series there is a total of 1620 genes that we considered DE in at least one time-series; these DE gene profiles and the motifs located in the genome by a *de novo* search were used in the factor model analysis.

### Motif search:dyads

We searched the *S. coelicolor* genome for statistically over represented dyad type motifs, i.e., binding sites with two conserved sequences and a variable non-conserved spacer between them using the method described in (24,25). Within the upstream 300 bp we identified 2120 potential motifs (with conserved sequences of length 4 and 5 and a spacer length lying between 4 and 20 bp) across the 7769 genes [Uniprot-GOA annotation (34)]. A further subtlety arises here because of the high GC content of *S. coelicolor*; this reduces the information content in the motifs against more balanced nt genomes, especially for high GC motifs. Thus, the motifs with high GC content have a huge number of genome hits, much more than is realistic for a bacterial TF, [Supplementary Figure S7](#). Thus, in our final motif shortlist we removed any motifs that have a

very high number of genome hits (more than 300 operons) and high GC content (>75%). We filtered out motifs that obviously had no explanatory power for the transcriptome data, i.e., we restricted to motifs that were highly enriched in at least one of (i) the differentially expressed gene sets of TS1, 3 or 5, (ii) in the dynamic gene clusters of TS1, 3, or 5, or (iii) in a set of PhoP dependant genes obtained by a comparative analysis of TS1 and TS3 (i.e., genes which have a significant change in their time series variance between the two time series). This enrichment analysis was done at the level of operons (see ‘Methods’ section) using the operon definitions of (32). This left 55 motifs with an approximately Poisson distribution for the number of motifs per gene, [Supplementary Figure S9](#) with mean 0.525, the main deviation occurring at high motif counts where we find a few targets have a higher number of motifs than the Poisson distribution. Motif logos (a qualitative representation of the sequence signature) for all the motifs are shown in the [Supplementary Figures S17–S26](#).

### Modelling motif activity: a factor model

The motif search defined a regulatory network comprising 55 motifs and 551 potential target genes with 855 links, i.e., an average connectivity of 1.55 motifs per gene, each motif occurring on average 16 times, [Supplementary Figure S8](#). However, all binding sites may not be real, i.e., there may be false positives or sites may be inactive under our experimental conditions. Thus, to refine the network we used expression data to identify the active binding sites and their associated motifs. This was accomplished by using the factor model, Equation 1 constrained by the motif-binding site network above. Our application is more challenging than the original study on *E. coli* (6). We therefore had to modify the original model and MCMC inference algorithm to improve its performance on our data, see [Supplementary Data](#). The analysis is Bayesian, computing the (posterior) probability  $P(z_{ij} = 1 | \text{Data})$  of each motif–gene interaction being present based on the expression data, shortened to  $P(z_{ij} = 1)$  in the following, while also inferring the activity profiles  $p_{jt}$  of the potential regulator associated with each motif. In our model the prior probability on the connectivity is itself considered a variable (i.e., the indicator variable for a link between gene  $i$ , motif  $j$ ,  $z_{ij} \sim \text{Binomial}(\rho_j)$  is parametrized by  $\rho_j$  (motif specific), a random variable, with prior  $\rho_j \sim \text{Beta}(2,2)$ ; this contrasts to (6) who fixed  $\rho_j$  at  $\frac{1}{2}$ ). Throughout the article, *significant targets* for a given motif  $j$  will mean those targets for which the posterior link probability is greater than the prior, i.e.,  $P(z_{ij} = 1) \geq \rho_j$ . Inference of the model parameters was performed concurrently across all model parameters using an MCMC methodology ([Supplementary Data](#)).

The motif–gene links supported by our experimental time series were determined, [Supplementary Table 1](#). The average number of significant targets per motif is 0.958, compared to the original 1.55 targets per motif, [Supplementary Figure S8](#). A few of the motifs are even switched off altogether, e.g., Motif 51, [Supplementary](#)

Figure S16, indicating that our selection of motifs was probably sufficiently broad. The posterior values of  $\rho_j$  for each motif  $j$  are shown in Supplementary Figure S10, again indicating that there is heterogeneity among the motifs in their explanatory power. Thus, the expression data introduces a strong selection on the potential binding sites with only 61% of the potentially informative computationally determined binding sites being active in our data. This is despite the fact that we initially selected only strong matches in the genome-wide search of binding sites (using a high threshold, HMMER score = 16).

### Regulator activity profiles

The factor model predicts the activity profiles of the regulator associated with each motif, identifying when they are active in the respective experiments, Figure 1. There are some highly variable patterns, but also some commonality. For instance, there are a number of motifs with oscillations at the start of the time series and a class with gradual decay in all the time series, most of the latter also showing a slight dip in TS5 around the time of glutamate depletion suggesting that these may be related to the stringent response. The stringent response is very pronounced in TS5. A global decay pattern is not unexpected since the fermentation environment becomes more hostile over time as nutrients deplete and toxins accumulate. We grouped the activity profiles into clusters using hierarchical clustering on the profile correlations, see Supplementary Figure S11. A cut-off of  $r^2 = 0.6$  gave a good separation of patterns, grouping the profiles into 10 motif activity clusters, Figure 2. Some of the activity clusters comprise only single motifs (activity clusters 1, 6, 8 and 9), i.e., they have unique profiles across the

time points while other groups (activity clusters 2, 3, 4, 5, 7 and 10) contain more than one motif indicating that their associated regulators have similar activity profiles. For example, activity cluster 5 contains all the regulators that have oscillations in their profiles prior to nutrient depletion; these oscillations are more pronounced in TS3 than TS1 and TS5 possibly because of the slower growth in TS3 (not shown), while activity cluster 7 includes all regulators which have an activity profile matching the gene expression profile of *phoP* (phosphate response regulator), (27), i.e., their activity is significantly increased at the time of phosphate depletion in TS1 while showing no significant activity in TS3 (where *phoP* is knocked-out) and TS5 (where *phoP* is inactive, data not shown). Motif 22 in this activity cluster is the PhoP motif, comprising directed repeats of the PHO box (14–16).

Although the activity clusters look compact, Figure 2, the correlation among their target sets is very variable. For example, for the PhoP-like activity cluster 7, the profile is very similar for all four motifs of the activity cluster but they do not share targets among each other except for 1 between motifs 40 and 47, Table 1. Further, their motif signatures do not share much similarity as shown in Figure 3, although all have a common pattern—a dyad with a repeated nt in each word of the dyad.

In contrast, activity cluster 5 comprises motifs that not only share similar activity profiles but share most of their targets. Further, the motifs overlap in the upstream regions, Figure 4 and there is high level of similarity in the motif sequences, Supplementary Figure S21. Motif 3 within this activity cluster contains all the significant targets within the motifs of cluster 5, Table 2, suggesting there is in fact only one binding motif.

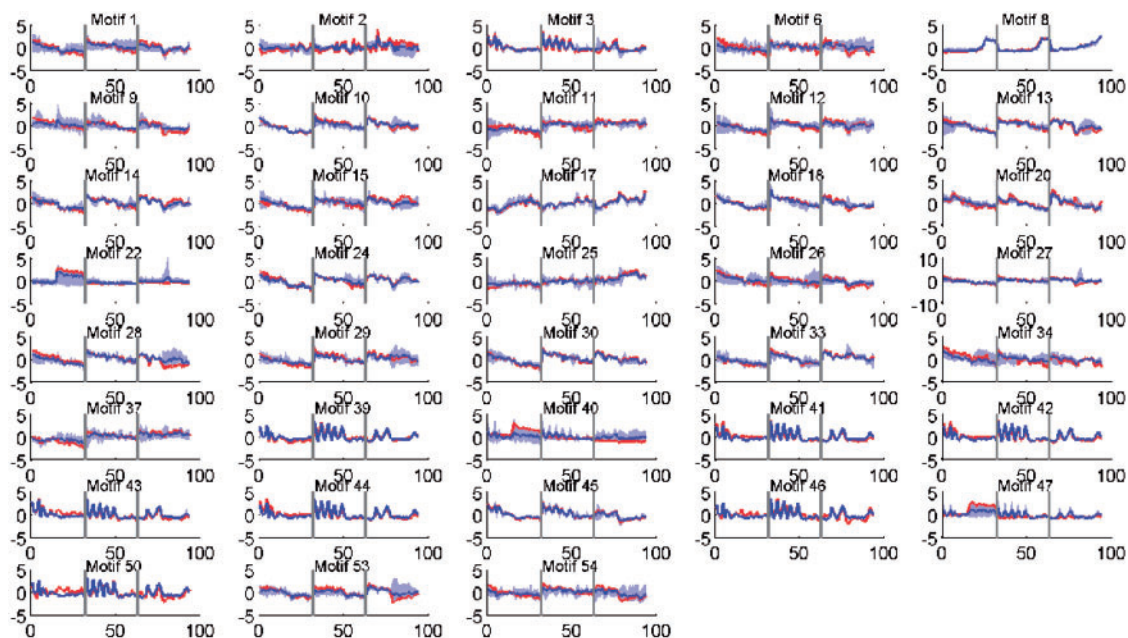


**Figure 1.** Activity profiles of selected motifs (those having > 50% correlation with their targets). Shown in red is the (mean) predicted activity of the motif using the factor model while in blue is the average expression profile of the (at most) top five significant targets. The shaded area (light blue) shows the range of the gene profiles of these top significant targets. Vertical lines (grey) separate the three time series, TS1, TS3 and TS5 respectively. Activity profiles of all motifs are given in Supplementary Data (Supplementary Figures S14 and S15).

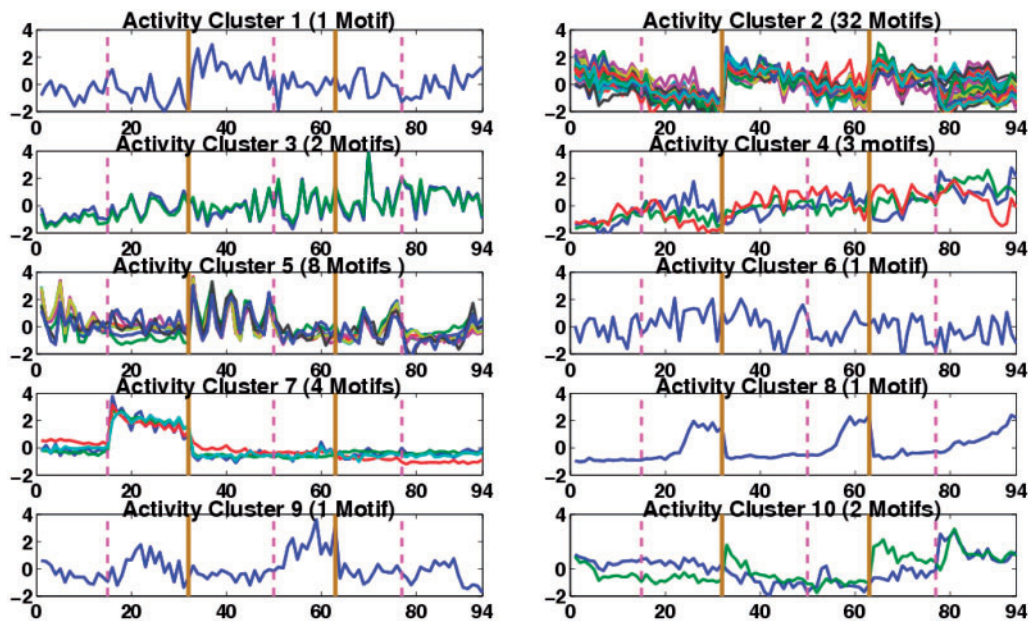


**Figure 2.** Predicted motif activity profiles grouped into 10 activity clusters. Individual motif patterns are distinguished by colour. In each of the plots, vertical solid lines (Brown) separate the three times series, TS1, TS3 and TS5 respectively, while the vertical dashed lines (Magenta) correspond to the nutrient depletion time in each time series.

**Table 1.** Proportion of targets shared by motifs in the PhoP activity cluster 7 (15 targets)

Motifs	21	22	40	47	Targets
21	1	0.0	0.0	0.0	5
22	0.0	1	0.0	0.0	4
40	0.0	0.0	1	0.2	5
47	0.0	0.0	0.5	1	2

Each entry corresponds to the proportion of common targets (defined as those having posterior  $P(z_{ij} = 1) > \rho_j$ ) among the motifs  $k$  (row) and  $j$  (column) relative the number of targets of motif  $k$ .

Members of the activity clusters 3, 4 and 10 do not have any common targets amongst themselves while the remaining activity clusters, except cluster 2, are only single motif activity clusters. Although cluster 2 contains most of the motifs (32 in total) there are a number of non-zero target overlaps in this activity cluster, [Supplementary Table 5](#); i.e., the proportion of common targets is predominantly low. The motifs in this activity cluster which do share targets, e.g., motifs 16 and 19, 4 and 5 as well as motifs 7, 28 and 29, suggest that this activity cluster comprises of the order of 28 distinct motifs, and associated regulators, that regulate the response to the degrading environment. Locations of the upstream binding sites for motifs in cluster 2 are shown in [Supplementary Figure S27](#) demonstrating that multiple motifs in the upstream regions are often well separated and thus distinct.

### Sensitivity analysis

The original motif search required a significance threshold to be chosen ( $P$  or  $q$ -value), thereby affecting how many motifs we utilize in the analysis. Of concern is whether we

have included sufficient motifs as explanatory variables or used too stringent a criterion such that the results are strongly dependent on the thresholds. Thus, we carried out a sensitivity analysis altering the enrichment threshold (from 9% to 10%) to increase the number of motifs to 72 from the previous 55, giving 688 genes with at least one motif. All other thresholds (HMMER threshold score of 16, GC content ( $\leq 75\%$ ), number of genome wide hits  $\leq 300$ ) were identical. Examining the (posterior) probability of common links between the two analyses gave a high level of correlation ( $r = 0.82$ ), [Figure 5](#). Out of a total of 855 a priori common links, there is agreement on the majority of the links in both cases, i.e., 448 significant links in both cases and 283 links which are switched off in both while there are only 124 links which are significant in one case while switched off in the other, [Figure 5](#). Further, the average number of posterior significant links per motif for the motifs in this analysis is 52% as compared to 56% in the original analysis. Out of the 55 common motifs, the number of inactive motifs (for which no posterior link is significant) was 2, respectively 3 in the larger/smaller runs. Of the additional 17 motifs of the larger run, one is inactive. We also clustered the predicted activity profiles of the 72 motifs into 9 clusters ( $r^2 = 0.5$ ), [Supplementary Figure S12](#), reproducing all the dominant patterns of the smaller run.

### DISCUSSION: COMPARISON WITH THE KNOWN REGULATORS

In order to determine possible identities of the regulators associated with each motif we used two methods. Firstly, we searched for regulators that are transcriptionally regulated under our experimental conditions by

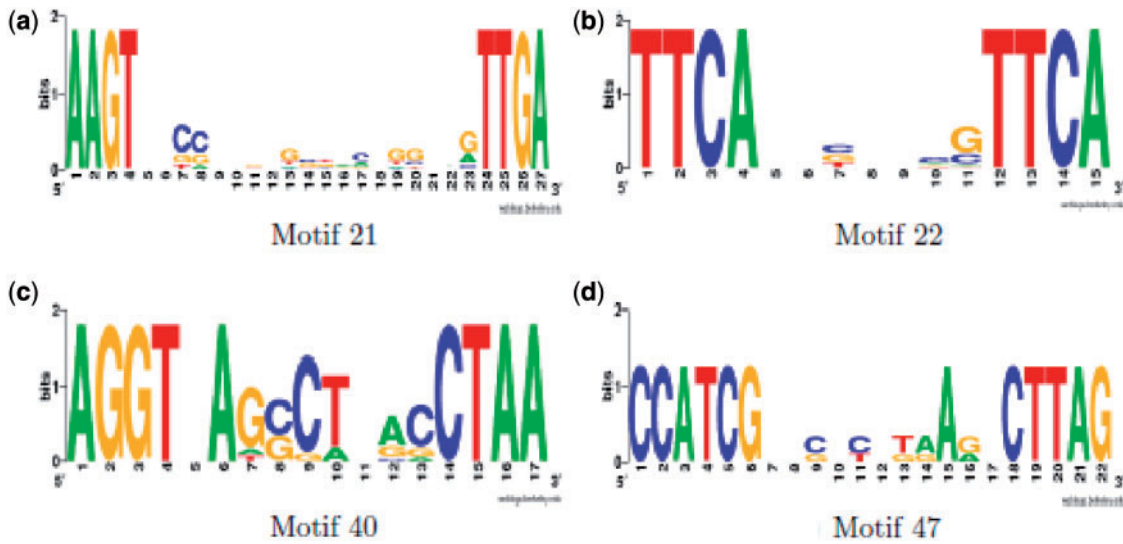


**Figure 3.** Motif Sequence logos for activity cluster 7 (15 target genes, 4 motifs). (a–d) Motif logos. Motif 22 (b) is the *S. coelicolor* directed repeat PHO box, albeit with the missing nt *G* at the start of the first conserved sequence. Motif logos generated using (35), <http://weblogo.berkeley.edu/>.

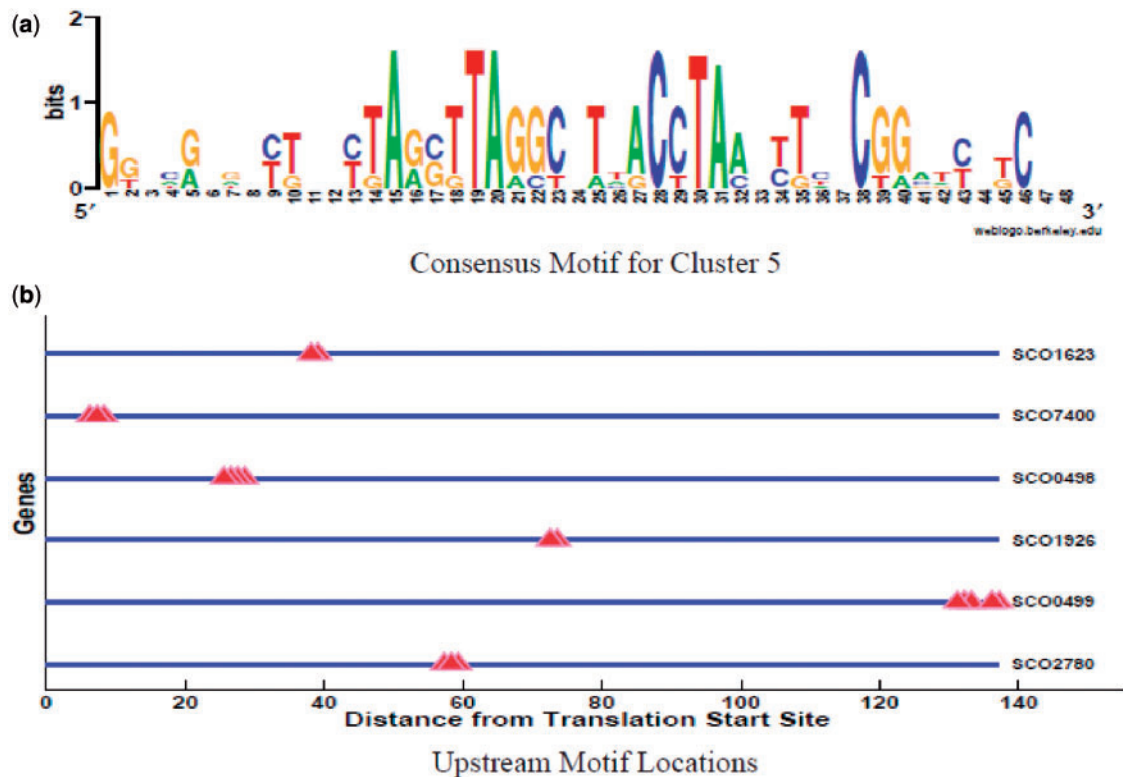


**Figure 4.** (a) Cluster 5 consensus logo created using the following procedure: The MEME suite (36) was used to construct a common underlying motif among the combined targets in this motif cluster. The logo in (a) was created from the multiple alignment of the sequences corresponding to the MEME output motifs plus some flanking sequences. This extended logo better represents the different overlapping motifs (Supplementary Figure S21) in this cluster than the MEME consensus logo generated from all targets in this activity cluster. (b) Locations of cluster 5 motifs in the upstream regions of the target genes (showing only those targets with at least two motif binding sites).

comparing our inferred motif activities against the expression profiles of a list of potential regulators in *S. coelicolor*, Supplementary Table 8. We calculated the distance between the activity profile for each motif against all the regulators in this list. Matches include a range of

bacterial regulators—transcriptional/response regulators, two component systems, DNA binding proteins etc. In Figure 6, we show a few of these matches. The top ten matches are given in Supplementary Table 3. Secondly, we compared our motifs against known

bacterial regulator motifs reported in the literature (through RegulonDB), and with the motif comparison tool STAMP (37). STAMP uses multiple databases for motif comparison including DPInteract for *E. coli* regulators (<http://arep.med.harvard.edu/dpinteract/index.html>). Each hit was then examined for a corresponding regulator in *S. coelicolor*. These analyses are discussed below for some individual motifs (also see [Supplementary Data](#) for Motif 51 (Zur/Fur homolog) and Motif 27 (PhoB homolog)).

### Motif 22: phosphate response regulator PhoP

Motif 22 (cluster 7 in [Figure 2](#)) has one of the most distinctive activity profiles with a dramatic transient increase in activity in TS1 at the time of nutrient (phosphate) depletion, while it is almost inactive (constant) in TS3 and TS5, see [Supplementary Figure S13](#). The motif is similar to the binding motif of PhoP comprising directed repeats of the PHO box (essentially GTTCA) (14–16), (although the first letter ‘G’ is lost/weak in each repeat,

**Table 2.** Proportions of significant targets (having posterior  $P(z_{ij} = 1) > \rho_j$ ) shared by motifs in activity cluster 5 (7 targets)

Motifs	3	39	41	42	43	44	46	50	Targets
3	1	0.14	0.14	0.14	0.42	0.14	0.14	0.14	7
39	1	1	1	1	1	1	1	1	1
41	1	1	1	1	1	1	1	1	1
42	1	1	1	1	1	1	1	1	1
43	1	0.33	0.33	0.33	1	0.33	0.33	0.33	3
44	1	1	1	1	1	1	1	1	1
46	1	1	1	1	1	1	1	1	1
50	1	1	1	1	1	1	1	1	1

Each entry corresponds to the proportion of common targets among the motifs  $k$  (row) and  $j$  (column) relative the number of targets of motif  $k$ .

[Figure 3](#)). Together this suggests that the regulator associated with motif 22 is PhoP. This is confirmed by its high confidence targets that are previously identified members of the PhoP regulon (14–16); SCO4142 which encodes a phosphate binding protein precursor within the high affinity phosphate transporter *pst* operon (SCO4139–42), SCO1393 which encodes for an acetoacetyl-CoA synthetase, SCO3790 a conserved hypothetical protein and SCO1906 a secreted protein. The activity profile has a high correlation to the three regulators PhoP (SCO4230), PhoU (SCO4228), AraC (SCO0466), ( $r = 0.83, 0.84$  and  $0.67$ , respectively). It is known that PhoP is transcriptionally activated under phosphate depletion (11,15,16) and regulates PhoU; hence explaining this high correlation.

We previously noted that three other motifs (21,39,46) in cluster 7 have very similar activity profiles but there are negligible common targets. Examination of the targets of motif 21 in activity cluster 7 reveals that one of the binding sites is within the upstream region of the diverging genes SCO4873 and SCO4874, i.e., within the genomic cluster (SCO4873–4882) of the *pho* regulon involved in the phosphate-free biosynthesis of secondary polymers of the cell wall (27), a known target of PhoP. Motif 40 has SCO4228, SCO4229 as targets, also known to be in the PhoP regulon (the phosphate two component system *phoURP* itself). However, these are the only targets that can be linked to the PhoP regulon reported in; i.e., the other nine targets are not known to be in the PhoP regulon. These targets also show occasional dynamics in TS3 and TS5 distinguishing them from those of motif 22, [Supplementary Figure S13](#). Further, a search for common motifs using MEME (36) within the combined targets of the motifs in this cluster found a PHO box as a consensus motif in the upstream regions of 6 of the 15 targets of cluster 7, [Supplementary Table 6](#), which include three out of four targets of motif 22, two out of five targets

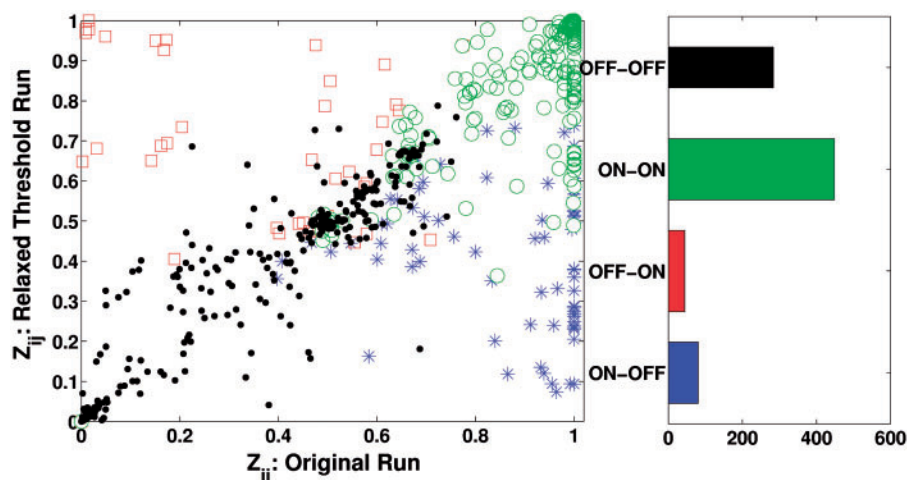


**Figure 5.** Robustness analysis. The posterior probabilities  $P(z_{ij} = 1)$  for all common motifs  $j$  and genes  $i$  are plotted for the two enrichment thresholds, 9% (Original) and 10%. All common motifs/genes between the two cases are plotted. Four subcategories are shown: blue asterisks for links which are ON (Significant) in First run and OFF (Not significant) in second, red squares show links which are OFF in first run and ON in second, green circles represent those links which are ON in both experiments while black point markers correspond to the links which are switched off in both cases. The right panel shows the number of links in each of the four categories of links in this comparison.

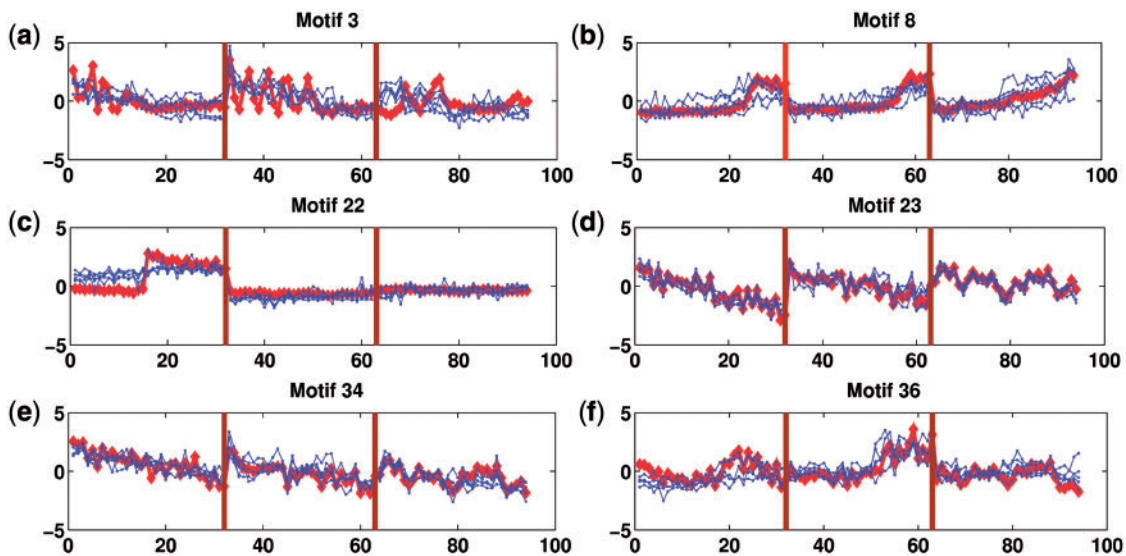


**Figure 6.** Comparison of six of our predicted motifs (red) with their 5 best matching known regulators (blue) in *S. coelicolor* (vertical lines separate the three times series, TS1, TS3 and TS5 respectively). Matching profiles are ascertained by using an Euclidean distance metric. These top hits are, (a) motif 3: XRE family DNA binding protein (SCO6770 which contains HTH3 Helix-turn-helix domain), putative TetR family regulatory protein (SCO4313) and a TetR family transcriptional regulator (SCO0622), a LacI family transcriptional regulator (SCO0062) as well as a sig15 sigma factor (SCO3068), (b) motif 8: SARP family regulator ActII-ORF4 (actinorhodin cluster regulator SCO5085), Afsr2 sigma like protein (SCO4425), ActII-1 putative TetR family transcriptional regulatory protein (SCO5082), an AraC family regulatory protein (SCO5017), and LuxR (*absR2*) regulatory protein (SCO6993), (c) motif 22: a response regulator PhoP (SCO4230) and AraC family transcriptional regulator (SCO0266), and MarR family regulatory protein (SCO0940), among others, (d) motif 23: DNA binding protein BldD (SCO1489), AraC family transcriptional regulator (SCO2792), Glk glucokinase (SCO2126) as well as transcriptional regulatory protein GlnR (SCO4159), (e) motif 34: MarR, MerR regulatory proteins (SCO5405, SCO2105) and TetR (SCO3129) family transcriptional regulators and a conserved hypothetical protein (SCO4639) as well as an anti Sigma factor (SCO7324), (f) motif 36: Matches to this motif include important transcriptional and response regulators like (SARP family) RedD (SCO5877) and RedZ (SCO5881) and a LuxR2comp two component regulator (SCO5785).

(SCO4873 and SCO4884) of motif 21 and SCO4229 (encoding the sensor kinase PhoR). Despite these differences in the performance of computational motif prediction methods, this analysis gives support to the suggestion that PhoP does not regulate all these targets and our original motif decomposition indicating multiple regulators is essentially correct, [Table 1](#). This is consistent with an independent analysis of this data that suggests that there is a PhoP-independent phosphate response (M. Juarez *et al.*, submitted for publication).

#### Cluster 5: the siderophores

The second rich dynamic pattern comprises eight motif activity profiles that group into activity cluster 5, [Figure 2](#), activity profiles that oscillate prior to nutrient depletion with TS3 and TS5 exhibiting the strongest oscillations. There is high overlap in their significant targets (all having motif 3) while the motifs have high levels of similarity, [Supplementary Figure S21](#). Further, motifs are closely clustered in the upstream regions of all targets (for genes having more than one binding site), [Figure 4](#). This indicates that these motifs are different overlapping versions of same underlying motif. We created a consensus sequence logo for this cluster using MEME (36), [Figure 4](#).

The target profile strongly suggests that this motif is the regulatory binding site for the siderophores and other iron-related genes. Among the 7 significant targets in this cluster we find 3 of the 18 siderophore genes, i.e., SCO0498, SCO2780 (putative secreted protein), and

SCO7400. However, the siderophores are organized into operons, specifically SCO0494-97 and SCO2783-85 (32); the targets SCO0498 and SCO2780 lie upstream of these two operons respectively, indicating that our targets probably include more than 1/2 of the siderophore genes. In fact SCO0498 (*cchB*) encodes an acyl transferase peptide monooxygenase of the coelichelin biosynthesis cluster (38); in *S. coelicolor* coelichelin acts as a siderophore. Further, *cchB* is regulated by PhoP under phosphate-limited conditions (16) and is a target of the  $\sigma^R$  regulon (39). The other four targets are SCO0499 (putative formyltransferase), SCO5999 (aconitase), SCO1926 (putative DNA-binding protein) and SCO1623 (conserved hypothetical protein). The *Streptomyces* aconitases belong to the Iron-Regulatory-Protein/AcnA family, while the aconitase AcnA of *S. viridochromogenes* possesses regulatory function within iron metabolism (40). Thus, there is a high density of iron-related genes among the targets of cluster 5.

Transcriptional oscillations have been previously reported in iron homeostasis in *E. coli*, including the observation of damped oscillations in the siderophores, (41). The hypothesized mechanism is through a coupling of iron transport regulating Fur binding. If the mechanism of the oscillations is similar, i.e., exponential growth in our fermentors leads to an iron concentration down shift that induces oscillation in the iron sensing circuit, then this suggests that this motif is that for the Fur homologue in *S. coelicolor*, *furS* [SCO0561, (42)]. Of note, we failed to

find a putative regulator with similar dynamics, consistent with regulation through iron binding. Further, the motif is unknown, although we did find a Zur/Fur motif homologue (Motif 51), see [Supplementary Data](#).

#### Motif 6: CRP family

Motif 6, a palindrome in activity cluster 2, looks identical to a bacterial motif for the CRP family of regulators (RegulonDB), [Figure 7](#). These proteins play a key role in bacterial stress responses (43). A putative CRP transcriptional regulator in *S. coelicolor* is SCO7543 (<http://strepdb.streptomyces.org.uk>). Since the activity profile has little distinguishing structure there were many hits with expression profiles of putative regulators, [Supplementary Table 3](#), we are therefore unable to identify potential transcriptionally regulated CRP family regulators associated with motif 6. The 10 targets of this motif include the acetyltransferase gene (SCO1864), the cytochrome oxidase gene (SCO3945), the ferredoxin gene (SCO5135) and some conserved hypothetical proteins. We used a gel-shift assay to obtain preliminary experimental confirmation for the most promising targets of this motif. We detected strong gel-shifts in SCO3320, SCO3945, SCO4562, see [Supplementary Figure S5](#), while there was no shift in corresponding control sequences.

#### Motif 35: analogues of *E. coli* regulator LexA

Motif 35 of cluster 2 (8 targets), a directed repeat motif, has a predicted generic decay of activity over all three time series with a sharp inhibition after nutrient depletion in TS1 and at depletion in TS5, recovering temporarily in the latter. Alternatively, the patterns after depletion may be viewed as evidence of oscillations, especially in TS3 and TS5. Thus, it is distinct from the gradual decay in the majority of motifs in activity cluster 2. There was a significant match of the motif (using STAMP) with that of LexA, [Figure 8](#), a known transcriptional repressor in *E. coli*, ( $P$ -value =  $6.24e^{-04}$ ). The analogue in *S. coelicolor* is also called LexA by sequence homology. We conclude that motif 35 is the LexA binding motif, while the correlation between the inferred motif activity profile and *lexA* expression is 0.60 indicating some degree of transcriptional control. The eight targets of motif 35 are SCO5085 (ActII-ORF4, actinorhodin cluster activator protein), SCO5646 (probable solute binding lipoprotein), SCO5737 (*gpsI* guanosine pentaphosphate synthetase), SCO4662 (*tufI* elongation factor TU-1), SCO3961 (*serS* Seryl-tRNA synthase), SCO5169 (putative ATP-binding protein), SCO5899 (hypothetical protein), and SCO3089 (putative ABC transporter ATP-binding protein).

#### Motifs 8 and 36: antibiotic synthesis

Motifs 8 and 36 are similar directed repeat motifs, but the former has a strongly structured activity profile, the latter a substantially weaker one, [Figure 9](#). The activity profile for motif 8 shows a distinct pattern with delayed activation relative to nutrient depletion, an activation that is slower in TS5. The targets include part of the actinorhodin synthesis cluster suggesting that this motif corresponds to the associated SARP (ActII-ORF4, SCO5085); this is

consistent with the high correlation of the activation profile with this gene,  $r = 0.949$ . Specifically, we have as targets two neighbouring genes (SCO5071 and SCO5072) on opposite strands, while SCO5072 is upstream of the genes SCO5073-5080 on the same strand and constitutes part of ACT cluster (27). Other targets in the ACT cluster are SCO5086 (ketoacyl reductase), SCO5087 (actinorhodin polyketide beta-ketoacyl synthase alpha subunit), and SCO5091 (cyclase). For motif 36, one of its target genes SCO5888 (*redP*) is upstream of a large cluster of genes (SCO5889-SCO5898) which comprise part of the undercylprodigiosin (Red) cluster. Further, *redD*, *redZ* are within the top 5 regulatory genes that have an expression profile which correlates with the activity profile, ( $r = 0.75, 0.72$  for *redD* and *redZ* respectively), [Figure 6](#), although the average correlation of motif 36 with its targets is poor ( $r = 0.0245$ ), [Figure 9](#). This suggests that motif 36 may be the motif for RedD (SCO5877), the regulatory cascade occurring through  $Z \rightarrow D \rightarrow red$  biosynthesis (SCO5886-5897), the pathway from *afsS* to *redZ* being unknown (44). Other targets of motif 36 which are not part of Red cluster are SCO4947 (nitrate reductase alpha chain NarG3), SCO3928 (putative thiamine biosynthesis protein), SCO1245 (adenosylmethionine-8-amino-7-oxononanoate amino transferase), SCO7403 (putative membrane protein), and SCO0902 (hypothetical protein). The structure of the motifs also supports the suggestion that these correspond to binding sites for SARPs; they have a periodicity of 11 nt corresponding to a complete turn of the DNA, while motif 8 has the previously identified distinctive TCGA pattern (19).

## CONCLUSION

We present a new methodology for the analysis of transcriptomic data in poorly studied organisms that integrates expression data with the genome sequence. The requirements for using our technique are low, only requiring a sequenced genome in which motifs can be detected, and a sufficiently informative expression data set comprising either multiple time series and/or steady state data. In contrast to many other integration methods, e.g., (45), a training set is not required. We applied our method to *S. coelicolor*, a model organism in the actinomycetes examining expression data during nutrient depletion (27,28 and M. Juarez *et al.*, Submitted for publication). We found 10 distinct patterns of 'motif' activity among the 55 motifs analysed (based on 94 arrays, 3 time series), [Figure 2](#). The dominant pattern (activity cluster 2) was a gradual decay comprising 32 motifs, although there were some differences in the detail of the profiles within this activity cluster, [Figures 2, 7 and 8](#), particularly at nutrient depletion. Given the lack of target overlaps we suggest that there are multiple regulators within this cluster with similar activity; separating these regulators would require additional data under conditions in which they are differentially activated. There were three highly distinctive activity patterns that are similar to the *phoP* expression profile (activity cluster 7),

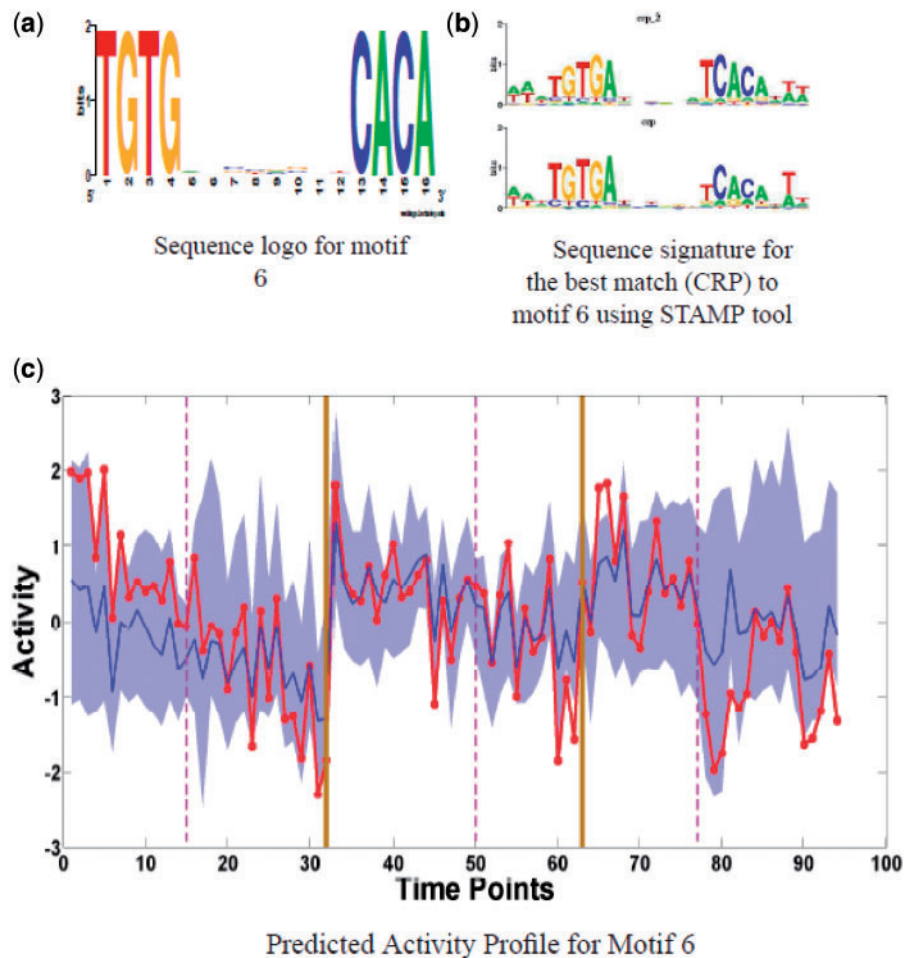


**Figure 7.** Motif 6 (CRP): (a) Sequence logo for motif 6. (b) Sequence logos for two bacterial CRP family regulators which are very similar to motif 6 with  $P$ -values of  $1.89e^{-10}$  and  $6.1e^{-08}$ . (c) Predicted Activity profile (red) along with the expression range (filled area with mean in blue) of the target genes. Vertical solid lines (Brown) separate three time series, TS1, TS3 and TS5 respectively while the vertical dashed lines (Magenta) correspond to the nutrient depletion time in each time series.

Figure 2, which included the PHO box directed repeat motif (and three others), a secondary metabolism biosynthesis profile (activity cluster 8 with targets that include the *act* cluster), Figures 2 and 9 and an oscillatory activity profile (activity cluster 5, that includes the siderophores in their targets), Figure 2. We made tentative predictions of the identity of the associated regulators. Our method successfully detected some known regulators, in particular PhoP and its PHO box, and the antibiotic SARPS *ActII-ORF4*, *RedD/Z*. Further, we identified the possible motif of the CRP regulator SCO7543. The correlation of the inferred activity of these motifs with the regulator's gene expression indicates whether it is transcriptionally regulated or is predominantly post-translationally regulated.

Preliminary experimental confirmation of some of our results was obtained by using gel-shift assays. These assays only provide evidence that there is a protein bound to the upstream region tested, and can not directly prove that the predicted motif is responsible. We found strong evidence of protein binding for targets containing motifs 6, 19, 20 and 25, Supplementary Figure S5 and Supplementary

Table 7. We also found evidence of binding for SCO0079 with *S. coelicolor* M145 cell lysate from S-medium (48 h); SCO0079 was a prediction under an earlier analysis for binding Motif 6 but removed later during the enrichment filtering step. Thus, altogether from 26 DNA sequences that were tested in EMSAs, five were identified to be specifically retarded (under a 500-fold excess dilution of unlabelled DNA), while no retardation occurred for any of the negative controls. The reason why the success rate is so low may be because of the experimental conditions. In such assays, purified binding protein is normally applied in appropriate concentrations to the respective target DNA but since we do not know the binding protein, we used cell lysate. Thus, the concentration of the binding protein in the *S. coelicolor* cell lysates may be low or the effector absent under the current conditions. Therefore, although the confirmation rate was low, we consider this as sufficient evidence to demonstrate that the analysis method is able to detect biologically relevant targets, and sufficient to motivate further analysis using more sophisticated, and challenging techniques that are able to identify the bound protein.

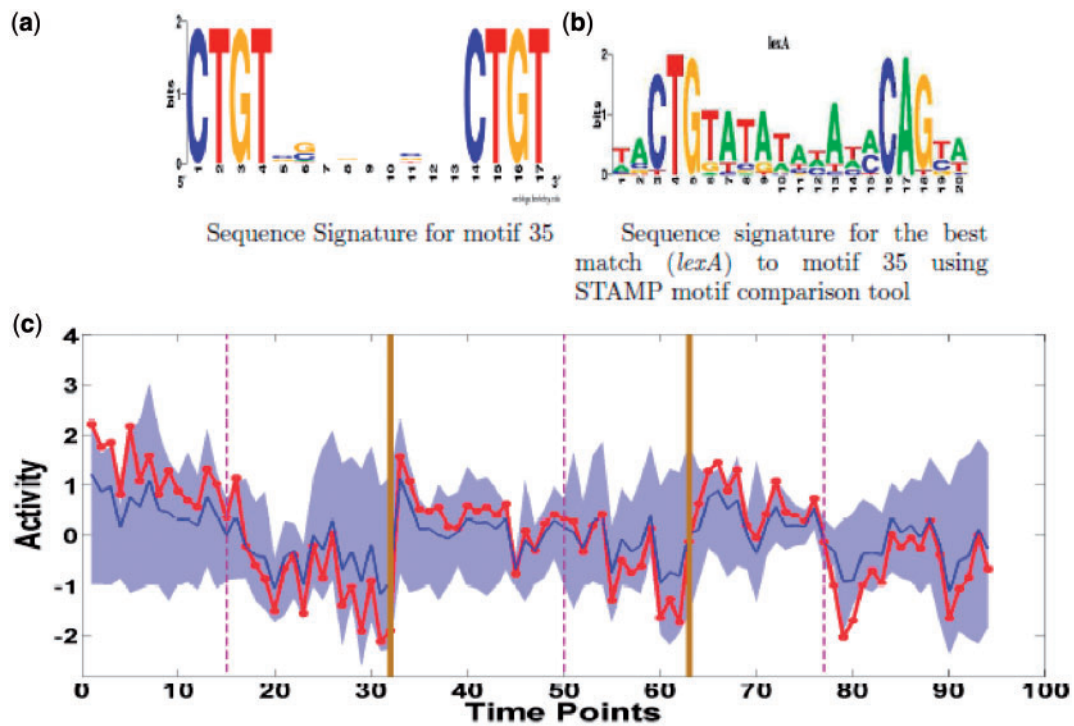


**Figure 8.** Motif 35 (*LexA*). (a) Sequence logo for motif 35 (b) Sequence logo for bacterial regulator *lexA* which is found as a best match to motif 35. (c) Predicted Activity profile (red). Annotation as Figure 7.

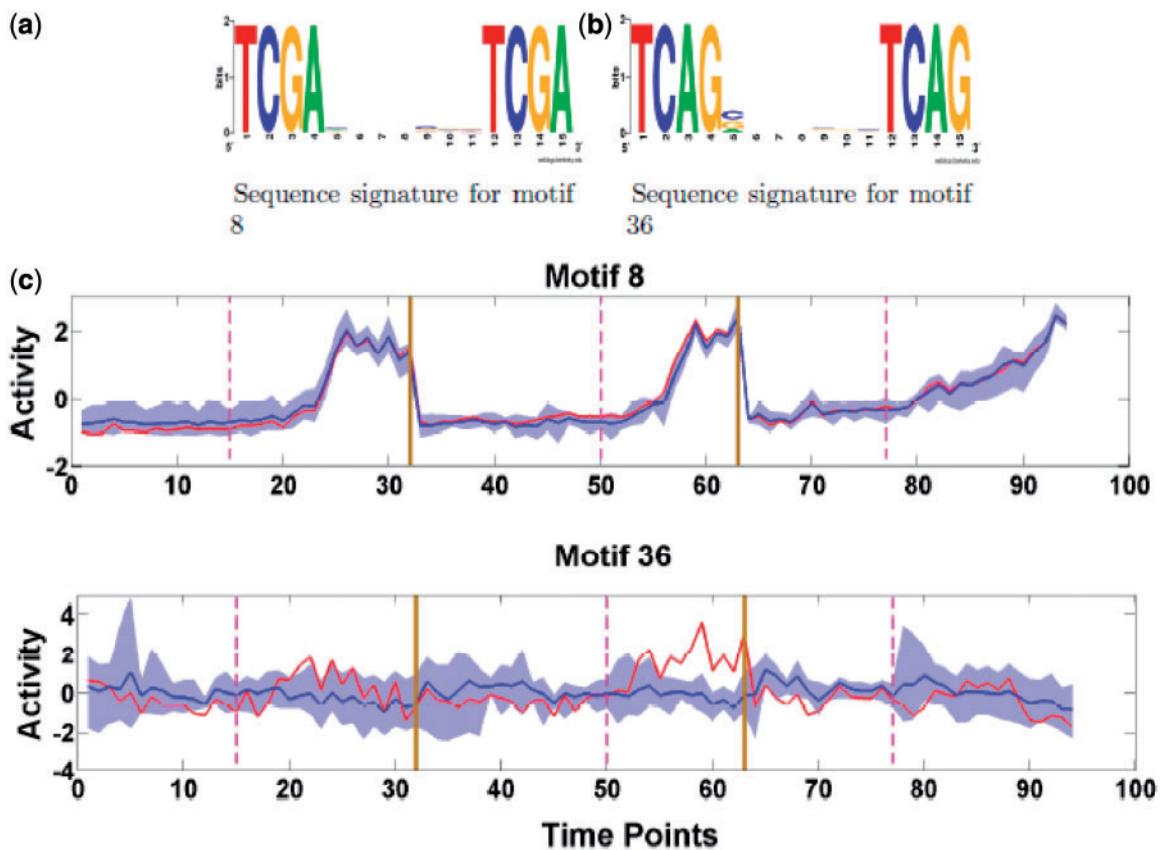


**Figure 9.** Antibiotic synthesis: (a) Sequence logo for motif 8. (b) Sequence logo for motif 36. (c) Predicted Activity profile (red) for motif 8 and 36. Annotation as Figure 7.

Our analysis identified key regulatory profiles and potential regulators in each of the experimental time-series. The wt response to phosphate depletion (TS1) is dominated by the exceptional strong activity cluster 7 pattern, the associated regulators being specific to this TS. This cluster includes the PhoP directed repeat PHO box binding site (motif 22), although this motif was present in only 1/2 the targets of this cluster. Our analysis therefore suggests that there are multiple regulators besides PhoP with similar profiles, which may be either downstream of the signalling cascade initiated by PhoP, or in parallel. Under glutamate depletion in the wt (TS5) we found a number of motifs with activity localized to nutrient depletion, and weak, or unresponsive to phosphate depletion in TS1/3. This suggests that motifs 6 (homologous to the CRP motif), 12, 13, 15, 25, 38, 54 correspond to specific cascades for carbon or nitrogen limitation, while a number of motifs have an inferred localized activity at/around both phosphate and glutamate depletion in wt suggesting a common stress response: this includes motifs 26, 27 and 35 (homology to *E. coli* LexA motif). Finally, we found a couple of activity profiles localized at phosphate depletion in the *phoP* KO: including motifs 11, 29, 33, motif 36 showing a phosphate response in TS1 & 3, while motifs 1, 14, 53 show activity in all time-series at depletion. This analysis indicates that the wt response to phosphate depletion is highly coordinated, primarily through PhoP, while response to glutamate depletion has considerable diversity with a rich range of activity profiles. The weakest signals were found in the *phoP* KO under phosphate depletion; a small number specific to this case were found, and a couple in common with glutamate depletion. This indicates that in absence of a PhoP response to deal with low phosphate, both a new specific response and a common response to glutamate depletion are triggered.

## SUPPLEMENTARY DATA

Supplementary Data are available at NAR Online: Supplementary Tables 1–8, Supplementary Figures S1–S28, Supplementary Methods, Supplementary Results and Supplementary References [46–53].

## ACKNOWLEDGEMENTS

Names and contacts of the members of the STREAM consortium can be found at <https://www.wsbc.warwick.ac.uk/groups/sysmopublic>. We thank J. Moore for bioinformatic support.

## FUNDING

Biotechnology and Biological Sciences Research Council (BBSRC), UK, grant number BB/FF003498/1, awarded through the ERA-NET SysMO initiative. (to M.I.); Higher Education Commission of Pakistan in collaboration with Dow University of Health Sciences, Karachi, Pakistan, and the ERA-IB Immunotech project (0315931) to R.A. Experimental data was generated under

STREAM, an international consortium funded under the ERA-NET SysMO initiative (Systems Biology of Microorganisms) <http://www.sysmo.net>. Funding for open access charge: Biotechnology and Biological Sciences Research Council (BBSRC).

*Conflict of interest statement.* None declared.

## REFERENCES

- Ross, P.L., Huang, Y.N., Marchese, J.N., Williamson, B., Parker, K., Hattan, S., Khainovski, N., Pillai, S., Dey, S., Daniels, S. *et al.* (2004) Multiplexed protein quantitation in *Saccharomyces cerevisiae* using amine-reactive isobaric tagging reagents. *Mol. Cell. Proteomics*, **3**, 1154–1169.
- Shadforth, I.P., Dunkley, T.P.J., Lilley, K.S. and Bessant, C. (2005) i-Tracker: for quantitative proteomics using iTRAQ. *BMC Genomics*, **6**, 145, doi:10.1186/1471-2164-6-145.
- Gao, F., Foat, B.C. and Bussemaker, H.J. (2004) Defining transcriptional networks through integrative modeling of mRNA expression and transcription factor binding data. *BMC Bioinformatics*, **5**, doi:10.1186/1471-2105-5-31.
- Ucar, D., Beyer, A., Parthasarathy, S. and Workman, C.T. (2009) Predicting functionality of protein-DNA interactions by integrating diverse evidence. *Bioinformatics*, **25**, i137–i144.
- Liao, J., Boscolo, R., Yang, Y., Tran, L.M., Sabatti, C. and Roychowdhury, V.P. (2003) Network component analysis: reconstruction of regulatory signals in biological systems. *PNAS*, **100**, 15522–15527.
- Sabatti, C. and James, G.M. (2006) Bayesian sparse hidden components analysis for transcription regulation networks. *Bioinformatics*, **22**, 739–746.
- Sanguinetti, G., Lawrence, N.D. and Rattray, M. (2006) Probabilistic inference of transcription factor concentrations and gene-specific regulatory activities. *Bioinformatics*, **22**, 2775–2781.
- Honkela, A., Girardot, C., Gustafson, E.H., Liu, Y.H., Furlong, E.E., Lawrence, N.D. and Rattray, M. (2010) Model-based method for transcription factor target identification with limited data. *Proc. Natl Acad. Sci. USA*, **107**, 7793–7798.
- Khanin, R., Vinciotti, V., Mersinias, V., Smith, C.P. and Wit, E. (2007) Statistical reconstruction of transcription factor activity using Michaelis-Menten kinetics. *Biometrics*, **63**, 816–823.
- Pournara, I. and Wernisch, L. (2007) Factor analysis for gene regulatory networks and transcription factor activity profiles. *BMC Bioinformatics*, **8**, 61.
- Martin, J.F. and Liras, P. (2010) Engineering of regulatory cascades and networks controlling antibiotic biosynthesis in *Streptomyces*. *Curr. Opin. Microbiol.*, **13**, 263–273.
- Rokem, J.S., Lantz, A.E. and Nielsen, J. (2007) Systems biology of antibiotic production by microorganisms. *Natural Prod. Rep.*, **24**, 1262–1287.
- Novotna, J., Vohradsky, J., Berndt, P., Gramajo, H., Langen, H., Li, X.M., Minas, W., Orsaria, L., Roeder, D. and Thompson, C.J. (2003) Proteomic studies of diauxic lag in the differentiating prokaryote *Streptomyces coelicolor* reveal a regulatory network of stress-induced proteins and central metabolic enzymes. *Mol. Microbiol.*, **48**, 1289–1303.
- Sola-Landa, A., Rodríguez-García, A., Apel, A.K. and Martín, J.F. (2008) Target genes and structure of the direct repeats in the DNA-binding sequences of the response regulator PhoP in *Streptomyces coelicolor*. *Nucleic Acids Res.*, **36**, 1358–1368.
- Rodríguez-García, A., Sola-Landa, A., Apel, A.K., Santos-Beneit, F. and Martín, J.F. (2009) Phosphate control over nitrogen metabolism in *Streptomyces coelicolor*: direct and indirect negative control of *glnR*, *glnA*, *glnII* and *antB* expression by the response regulator PhoP. *Nucleic Acids Res.*, **37**, 3230–3242.
- Rodríguez-García, A., Barreiro, C., Santos-Beneit, F., Sola-Landa, A. and Martín, J.F. (2007) Genome-wide transcriptomic and proteomic analysis of the primary response to phosphate limitation in *Streptomyces coelicolor* M145 and in a  $\Delta$ *phoP* mutant. *Proteomics*, **7**, 2410–2429.

17. Rigali, S., Titgemeyer, F., Barends, S., Mulder, S., Thomae, A.W., Hopwood, D.A. and van Wezel, G.P. (2008) Feast or famine: the global regulator DasR links nutrient stress to antibiotic production by *Streptomyces*. *EMBO Rep.*, **9**, 670–675.
18. Folcher, M., Gaillard, H., Nguyen, L.T., Nguyen, K.T., Lacroix, P., Bamas-Jacques, N., Rinkel, M. and Thompson, C.J. (2001) Pleiotropic functions of a *Streptomyces pristinaespiralis* autoregulator receptor in development, antibiotic biosynthesis, and expression of a superoxide dismutase. *J. Biol. Chem.*, **276**, 44297–44306.
19. Wietzorrek, A. and Bibb, M. (1997) A novel family of proteins that regulates antibiotic production in streptomycetes appears to contain an OmpR-like DNA-binding fold. *Mol. Microbiol.*, **25**, 1177–1184.
20. Sheldon, P.J., Busarow, S.B. and Hutchinson, C.R. (2002) Mapping the DNA-binding domain and target sequences of the *Streptomyces peucetius* daunorubicin biosynthesis regulatory protein, DnrI. *Mol. Microbiol.*, **44**, 449–460.
21. Paget, M.S., Kang, J.G., Roe, J.H. and Buttner, M.J. (1998)  $\sigma^R$  an RNA polymerase sigma factor that modulates expression of the thioredoxin system in response to oxidative stress in *Streptomyces coelicolor* A3(2). *EMBO J.*, **17**, 5776–5782.
22. Reuther, J. and Wohlleben, W. (2007) Nitrogen metabolism in *Streptomyces coelicolor*: transcriptional and post-translational regulation. *J. Mol. Microbiol. Biotechnol.*, **12**, 139–146.
23. Touzain, F., Schbath, S., Debled-Rensson, I., Aigle, B., Kucherov, G. and Leblond, P. (2008) SIGffRid: a tool to search for sigma factor binding sites in bacterial genomes using comparative approach and biologically driven statistics. *BMC Bioinformatics*, **9**, 73.
24. Studholme, D.J., Bentley, S.D. and Kormanec, J. (2004) Bioinformatic identification of novel regulatory DNA sequence motifs in *Streptomyces coelicolor*. *BMC Microbiology*, **4**, 14.
25. Li, H., Rhodius, V., Gross, C. and Siggia, E.D. (2002) Identification of the binding sites of regulatory proteins in bacterial genomes. *Proc. Natl. Acad. Sci. USA*, **99**, 11772–11777.
26. Robison, K., McGuire, A.M. and Church, G.M. (1998) A comprehensive library of DNA-binding site matrices for 55 proteins applied to the complete *Escherichia coli* K-12 genome. *J. Mol. Biol.*, **284**, 241–254.
27. Nieselt, K., Battke, F., Herbig, A., Bruheim, P., Wentzel, A., Jakobsen, Ø.M., Sletta, H., Alam, M.T., Merlo, M.E., Moore, J. et al. (2010) The dynamic architecture of the metabolic switch in *Streptomyces coelicolor*. *BMC Genomics*, **11**, doi:10.1186/1471-2164-11-10.
28. Waldvogel, E., Herbig, A., Battke, F., Amin, R., Nentwich, M., Nieselt, K., Ellingsen, T.E., Wentzel, A., Hodgson, D.A., Wohlleben, W. et al. (2011) The P<sub>III</sub> protein GlnK is a pleiotropic regulator for morphological differentiation and secondary metabolism in *Streptomyces coelicolor*. *Appl. Microbiol. Biotechnol.*, **92**, 1219–1236.
29. Angelini, C., Cutillo, L., De Canditiis, D., Mutarelli, M. and Pensky, M. (2008) BATS: a Bayesian user-friendly software for Analyzing Time Series microarray experiments. *BMC Bioinformatics*, **9**, 145.
30. Heard, N.A., Holmes, C.C. and Stephens, D.A. (2006) A quantitative study of gene regulation involved in the immune response of Anopheline mosquitoes: an application of Bayesian hierarchical clustering of curves. *J. Amer. Stat. Assoc.*, **101**, 18–29.
31. Bentley, S.D., Chater, K.F., Cerdeño-Tárraga, A.M., Challis, G.L., Thomson, N.R., James, K.D., Harris, D.E., Quail, M.A., Kieser, H., Harper, D. et al. (2002) Complete genome sequence of the model actinomycete *Streptomyces coelicolor* A3(2). *Nature*, **417**, 141–147.
32. Charaniya, S., Mehra, S., Lian, W., Jayapal, K.P., Karypis, G. and Hu, W. (2007) Transcriptome dynamics-based operon prediction and verification in *Streptomyces coelicolor*. *Nucleic Acids Res.*, **35**, 7222–7236.
33. Kieser, T., Bibb, M.J., Buttner, M.J., Chater, K.F. and Hopwood, D.A. (2000) *Practical Streptomyces Genetics*. John Innes Foundation, Norwich.
34. Barrell, D., Dimmer, E., Huntley, R.P., Binns, D., O'Donovan, C. and Apweiler, R. (2009) The GOA database in 2009—an integrated Gene Ontology Annotation resource. *Nucleic Acids Res.*, **37**, D396–D403.
35. Crooks, G.E., Hon, G., Chandonia, J.M. and Brenner, S.E. (2004) WebLogo: a sequence logo generator. *Genome Res.*, **14**, 1188–1190.
36. Bailey, T.L. and Elkan, C. (1994) Fitting a mixture model by expectation maximization to discover motifs in biopolymers. In: *Proceedings of the Second International Conference on Intelligent Systems for Molecular Biology*. AAAI Press, Menlo Park, California, pp. 28–36.
37. Mahony, S. and Benos, P.V. (2007) STAMP: a web tool for exploring DNA-binding motif similarities. *Nucleic Acids Res.*, **35**, W253–W258.
38. Barona-Gómez, F., Lautru, S., Francou, F.X., Leblond, P., Pernodet, J.L. and Challis, G.L. (2006) Multiple biosynthetic and uptake systems mediate siderophore-dependent iron acquisition in *Streptomyces coelicolor* A3(2) and *Streptomyces ambofaciens* ATCC 23877. *Microbiology*, **152**, 3355–3366.
39. Kallifidas, D., Thomas, D., Doughty, P. and Paget, M.S.B. (2010) The  $\sigma^R$  regulon of *Streptomyces coelicolor* A3(2) reveals a key role in protein quality control during disulphide stress. *Microbiology*, **156**, 1661–1672.
40. Schinko, E., Schad, K., Eys, S., Keller, U. and Wohlleben, W. (2009) Phosphinothricin-tripeptide biosynthesis: an original version of bacterial secondary metabolism? *Phytochemistry*, **70**, 1787–1800.
41. Amir, A., Meshner, S., Beatus, T. and Stavans, J. (2010) Damped oscillations in the adaptive response of the iron homeostasis network of *E. coli*. *Mol. Microbiol.*, **76**, 428–436.
42. Hahn, J.S., Oh, S.Y. and Roe, J.H. (2000) Regulation of the *furA* and *catC* operon, encoding a ferric uptake regulator homologue and catalase-peroxidase, respectively, in *Streptomyces coelicolor* A3(2). *J. Bacteriol.*, **182**, 3767–3774.
43. Körner, H., Sofia, H.J. and Zumft, W.G. (2003) Phylogeny of the bacterial superfamily of Crp-Fnr transcription regulators: exploiting the metabolic spectrum by controlling alternative gene programs. *FEMS Microbiol. Rev.*, **27**, 559–592.
44. Lian, W., Jayapal, K.P., Charaniya, S., Mehra, S., Glod, F., Kyung, Y.S., Sherman, D.H. and Hu, W.S. (2008) Genome-wide transcriptome analysis reveals that a pleiotropic antibiotic regulator, AfsS, modulates nutritional stress response in *Streptomyces coelicolor* A3(2). *BMC Genomics*, **9**, 56.
45. Zvir, I., Huang, H. and Groisman, E.A. (2005) Analysis of differentially-regulated genes within a regulatory network by GPS genome navigation. *Bioinformatics*, **21**, 4073–4083.
46. Okanishi, M., Suzuki, K. and Umezawa, H. (1974) Formation and reversion of streptomycetes protoplasts: cultural condition and morphological study. *J. Gen. Micro.*, **80**, 389–400.
47. Claessen, D., Rink, R., de Jong, W., Siebring, J., de Vreugd, P., Boersma, F.G., Dijkhuizen, L. and Wosten, H.A. (2003) A novel class of secreted hydrophobic proteins is involved in aerial hyphae formation in *Streptomyces coelicolor* by forming amyloid-like fibrils. *Genes Dev.*, **17**, 1714–1726.
48. Thompson, J.D., Higgins, D.G. and Gibson, T.J. (1994) CLUSTALW: improving the sensitivity of progressive multiple sequence alignments through sequence weighting, position specific gap penalties and weight matrix choice. *Nucleic Acids Res.*, **22**, 4673–4680.
49. Benjamini, Y. and Hochberg, Y. (1995) Controlling the false discovery rate: a practical and powerful approach to multiple testing. *J. Royal Stat. Soc. Series B (Methodological)*, **57**, 289–300.
50. Gilks, W.R. and Roberts, G.O. (1996) Strategies for improving MCMC. In: Gilks, W.R., Richardson, S. and Spiegelhalter, (eds), *Markov chain Monte Carlo in Practice*. Chapman and Hall, London, pp. 89–114.
51. Geyer, C.J. (1991) Markov chain Monte Carlo maximum likelihood. In: Keramidas, (ed.), *Computing Science and Statistics: Proceedings of the 23rd Symposium on the Interface*. Interface Foundation, Fairfax Station, pp. 156–163.
52. Altekar, G., Dwarkadas, S., Huelsenbeck, J.P. and Ronquist, F. (2004) Parallel Metropolis coupled Markov chain Monte Carlo for Bayesian phylogenetic inference. *Bioinformatics*, **20**, 407–415.
53. Patzer, S.I. and Hantke, K. (2000) The zinc-responsive regulator Zur and its control of the *znu* gene cluster encoding the ZnuABC zinc uptake system in *Escherichia coli*. *J. Biol. Chem.*, **275**, 24321–24332.